Minimizing Multiple Access Interference through Advanced Waveform Design in DS-CDMA

J. RAVINDRA BABU[1,*], K. SAI SANKAR[1], V. LAHARI[1], SK NOOR AHAMAD[1],
K. SRINIVAS[1], J. V. RAVI CHANDRA[2], J. V. RAVI TEJA[3], G. SRUJANA[1]
[1]E.C.E Department, P.V.P.,
Siddhartha Institute of Technology, Vijayawada,
INDIA

[2]CSE Department,
V. R. Siddhartha Engineering College,
Vijayawada,
INDIA

[3]Blur Matrix Software Solutions,
Hyderabad,
INDIA

**Corresponding Author*

Abstract: - DS/SSMA (Direct-sequence spread-spectrum multiple-access) technology has become a cornerstone of modern wireless communication infrastructure, enabling concurrent transmissions for multiple users over shared bandwidth. This study examines how multiple access interference (MAI) degrades DS/SSMA performance, with particular emphasis on the bit error rate (BER) metric. A simulation framework developed in MATLAB is employed to systematically assess the contributions of spreading code type, chip waveform selection, and code length under both synchronous and asynchronous operating conditions. Simulation outcomes reveal that Gold codes consistently yield lower BER than aperiodic random codes in synchronous configurations. In contrast, alternative chip waveform shaping techniques such as Blackman and Lanczos pulses offer minimal performance gains across both network synchronization modes.

Key-Words: - Direct-sequence spread spectrum, multiple access interference, bit error rate, spreading codes, wireless communication, Blackman and Lanczos pulses.

Received: March 16, 2026. Revised: May 19, 2026. Accepted: June 13, 2026. Published: October 30, 2026.

1 Introduction

The exponential growth of global wireless communication networks has placed mounting pressure on the design of multiple-access schemes capable of accommodating an ever-increasing population of simultaneous users. Direct-sequence spread-spectrum (DSSS) technology has emerged as a preferred solution in contemporary communication architectures, allowing multiple transmissions to coexist across common frequency bands. Nevertheless, as the number of active users rises, system performance degrades substantially due to the accumulating effect of multiple access interference (MAI) [1], [2], [3]. Consequently, a thorough understanding of how MAI governs system behavior is indispensable for advancing both spectral utilization and overall network capacity in present and forthcoming wireless standards [4], [5].

Considerable prior research has focused on characterizing MAI behavior in DS/SSMA architectures, largely relying on closed-form analytical derivations and statistical approximation methods. Although these theoretical frameworks offer meaningful foundational understanding, their applicability is constrained by oversimplified assumptions that disregard the complex interplay among system variables. Key factors influencing MAI—such as user load, spreading code properties, and sequence length—are rarely captured comprehensively within a single analytical model. Extending such models to incorporate additional variables typically demands extensive mathematical

restructuring, which significantly curtails their practical adaptability [6], [7], [8].

In response to the shortcomings of purely theoretical approaches, this investigation employs a computer simulation methodology to study MAI characteristics in DS/SSMA systems. The simulation paradigm allows systematic examination of a wide range of parameter combinations without the restrictions imposed by mathematical approximation. Furthermore, simulation-driven evaluation provides a more representative depiction of practical wireless scenarios, facilitating direct cross-validation against analytical predictions derived from established models [9], [10].

2 Signal and System Model

The data-modulated signal bi(t) associated with each individual user is mathematically expressed as:

$$b_i(t) = \sum_{n=-\infty}^{\infty} b_{i,n} P_{T_S}(t - nT_s) \quad (1)$$

where $b_{i,n}$ is a sequence of elements , $b_{i,n} \in [-1,1]$

and $P_T(*)$ denotes a unit-amplitude rectangular pulse spanning duration T_S, the symbol duration. Spreading code modulation $a_k(t)$ is defined as:

$$a_k(t)=\sum_{j=-\infty}^{\infty} a_j^{(k)} P_{T_C}(t - jT_C) \quad (2)$$

where $a_j^{(k)}$ is a sequence of elements for the k[th] user, $a_j \in [-1,1]$, each chip interval has duration T_c, and the spreading code period is $N*T_c$. In the majority of practical implementations, the chip pulse shape applied across each chip interval takes a rectangular form, as captured by $P_{T_C}(t - jT_C)$ in (2). One of

$$S_k(t)=\sqrt{2P} a_k(t) b_k(t) \cos(\omega_c t + \theta_k) \quad (3)$$

For the equal power cases considered here, $\sqrt{2P}$ represents the transmitted power of all signals, $\cos(\omega_c t + \theta_k)$ is the phase carrier of the k[th] user, ω_c is the modulation frequency and θ_k is the phase delay of the k[th] user

$S_k(t)= S_k(t)=$

$$\sum_{k=1}^{K} \sqrt{2P}\, a_k(t - \tau_k) b_k(t - \tau_k) \cos(\omega_c t + \emptyset_k) + n(t) \quad (4)$$

where τ_k and $\emptyset_k$ are the time delay and received phase, respectively, of the k[th] user. The noise term n(t) models thermal channel disturbances and is characterized as Additive White Gaussian Noise (AWGN) with a two-sided power spectral density of $N_o/2$. Throughout the derivations that follow, it is assumed that the desired user experiences neither propagation delay nor phase offset. Each interfering user exhibits a time delay, measured relative to the desired user, uniformly distributed within $[0,T_s]$ alongside a carrier phase offset uniformly distributed over $[0,2\pi]$. Under the special condition of a fully synchronous network, all interfering users are assumed to have identical timing with no delay offset.

$$Z_i = \int_0^T r(t) a_i(t) \cos(\omega_c t)\, dt. \quad (5)$$

Assuming $\omega_c >> T_s^{-1}$, the double-frequency term becomes negligible and can be discarded, allowing Z_i can be rewritten as

$$Z_i = \sqrt{\frac{P}{2}} \cdot \left\{ b_{t,0} T + \sum_{\substack{k=1 \\ k \neq i}}^{K} \left[b_{k,-1} R_{k,i}(\tau_k) + b_{k,0} \hat{R}_{k,i}(\tau_k) \right] . \cos \emptyset_k \right\} + \int_0^T n(t) a_i(t) \cos(\omega_c t) dt \quad (6)$$

where $R_{k,i}(\tau)$ and $\hat{R}_{k,i}(\tau)$ are defined as continuous-time, partial cross-correlation functions and expressed as

$$R_{ki}(\tau) = \int_0^T a_k(t - \tau) a_i(t)\, dt$$

$$\hat{R}_{k,i}(\tau) = \int_\tau^T a_k(t - \tau) a_i(t)\, dt \quad (7)$$

The partial cross-correlations $R_{ki}(\tau)$ and $\hat{R}_{k,i}(\tau)$ of(7) account for the mismatch between symbol transition boundaries of the desired user and the k[th] user resulting from the k[th] user's time delay and the k[th] user is an interferer. $R_{ki}(\tau)$ correlates the end of the first symbol of the k[th] user that falls within the desired user's symbol

interval, and $\hat{R}_{k,i}(\tau)$ correlates the beginning of the next subsequent symbol of the k[th] user which completes the rest of the desired user's symbol interval.

$R_{ki}(\tau)$ *and* $\hat{R}_{k,i}(\tau)$ can be written in terms of the discrete aperiodic cross-correlation function $C_{k,t}(l)$ defined as:

$$C_{k,i}(l) = \begin{cases} \sum_{j=0}^{N-1-l} a_j^{(k)} a_{j+1}^{i} & 0 \le l \le N-1 \\ \sum_{j=0}^{N-1+l} a_{j-1}^{(k)} a_j^{i} & 1-N \le l \le 0 \\ 0 & |l| \ge N. \end{cases} \quad (8)$$

Substituting $C_{k,i}(l)$ of (8) into (7) results in the following alternate expression for $R_{ki}(\tau)$ *and* $\hat{R}_{k,i}(\tau)$:

$$\hat{R}_{k,i}(\tau) = C_{k,i}(l)T_c + \left[C_{k,i}(l+1) - C_{k,i}(l)\right].(\tau - lT_c) \quad (9)$$

To establish the received signal-to-interference-plus-noise ratio (SINR), the power of the noise plus interfering signals is calculated as the variance of Z_i defined in (6) over one symbol interval and is given by:

$$Var\{Z_i\} = \left(\frac{P}{4T}\right)\sum_{\substack{k=1 \\ k\neq i}}^{K}\int_0^T \left(R_{k,i}^2(\tau) + \hat{R}_{k,i}^2(\tau)\right)d\tau + {N_o T}/{4}$$

$$= \left(\frac{P}{4T}\right)\sum_{\substack{k=1 \\ k\neq i}}^{K}\sum_{l=0}^{N-1}\int_{lT_c}^{(l+1)T_c} \left(R_{k,i}^2(\tau) + \hat{R}_{k,i}^2(\tau)\right)d\tau + {N_o T}/{4} \quad (10)$$

Here, the expectation operator is applied over the random variables $\emptyset_k, \tau_k$ and b_k. Since the intended user's data symbol is held fixed across the observation interval, equation (10) captures only the variance contributions attributable to AWGN and MAI. Inserting the $R_{ki}(\tau)$ *and* $\hat{R}_{k,i}(\tau)$ expressions derived in (9) into (10) yields the following condensed variance expression:

$$Var\{Z_i\} = \left(\frac{PT^2}{12N^3}\right)\left(\sum_{\substack{k=1 \\ k\neq i}}^{K} r_{k,i}\right) + {N_o T}/{4} \quad (11)$$

where

$$r_{k,i} = \sum_{k=1}^{N-1}\left\{C_{k,i}^2(I-N) + C_{k,i}(I-N)C_{k,i}(I-N+1) + C_{k,i}^2(I-N+1) + C_{k,i}^2(I) + C_{k,i}(I+1) + C_{k,i}^2(I+1)\right\} \quad (12)$$

The SINR is then determined by dividing $\sqrt{P/2T}$ by the rms noise of $\sqrt{\mathrm{Var}\{Z_i\}}$ yielding:

$$\mathrm{SINR} = \left[(6N^3)^{-1}\sum_{k=1}^{K} r_{k,i} + \frac{N_0}{2E_b}\right]^{-1/2} \quad (13)$$

As a practical aid for initial system dimensioning, expression (13) reduces to the following compact form when random spreading codes are assumed:

$$\mathrm{SINR} = \left\{\frac{K-1}{3N} + \frac{N_0}{2E_b}\right\}^{-1/2} \quad (14)$$

where the $(K-1)/(3N)$term arises from computing the ensemble average of the summation in (13) under the assumption of random spreading sequences. The standard bit error probability expression (P_B)applicable to an interference-free BPSK system is given by:

$$P_B = Q\left(\sqrt{\frac{2E_b}{N_0}}\right) \quad (15)$$

Using (14) an approximate P_B value can be calculated for a DS/SSMA system using (15) as:

$$P_B = Q(\mathrm{SINR}). \quad (16)$$

It is worth highlighting that when only a single user is active $(K = 1)$, expression (14) correctly reduces to the Q-function argument found in (15), confirming consistency with the standard single-user result

2.1 BER for Asynchronous and Synchronous Systems

By applying characteristic function analysis to

DSSS waveforms, expression (15) is reformulated through analytical derivation as:

$$\text{SINR} = \left\{\frac{K-1}{N} m_\psi + \frac{N_0}{2E_b}\right\}^{-1/2} \quad (17)$$

where $m_\psi = 1/3$when rectangular chip pulses are employed, and is further specified as:

$$m_\psi = T_c^{-3} \int_0^{T_c} R_\psi^2(\tau)\, d\tau = T_c^{-3} \int_0^{T_c} \hat{R}_\psi^2(\tau)\, d\tau \quad (18)$$

In (18) $R_\psi$and $\hat{R}_\psi$denote the partial autocorrelation functions corresponding to the selected pulse shape, which are formally expressed as:

$$\hat{R}_\psi(\tau) = \int_\tau^{T_c} \psi(t)\psi(t-\tau)\, dt \quad (19)$$

$$R_\psi(\tau) = \hat{R}_\psi(T_c - \tau).$$

The above derivation confirms that expression (14) is valid strictly for estimating SINR in the asynchronous operating mode with rectangular chip pulse shaping. Extending this analytical development further, a corresponding BER approximation applicable to synchronous DS/SSMA operation with rectangular chip waveforms takes the form

$$\text{SINR} = \left\{\frac{K-1}{N} + \frac{N_0}{2E_b}\right\}^{-1/2} \quad (20)$$

2.2 Chip Waveform Shaping

To mitigate the degrading impact of MAI in DS/SSMA systems, this section investigates how selecting non-rectangular chip waveform profiles can alter interference characteristics. The underlying rationale is that varying the chip pulse geometry modifies the cross-correlation properties among different users' spreading codes, potentially yielding lower interference levels. Six candidate pulse shapes are evaluated in this work: rectangular, half-sine, raised-cosine, Blackman, Kaiser, and Lanczos. Their respective mathematical representations are given as follows:

a) **Blackman**

$\psi(t) = k\,[\,0.42 - 0.5\cos(2\pi t / Tc)\,]\,u(t)$

b) **Half-sine**

$\psi(t) = \sqrt{2}\sin(\pi t / Tc)\,u(t)$

c) **Kaiser**

$\psi(t) = k * I_0(\beta\pi\sqrt{(1 - ((t - Tc/2)/Tc)^2)}) / I_0(\beta\pi) * u(t)$

d) **Lanczos**

$\psi(t) = k\,[\,\sin(2\pi t)/(2\pi t)\,]^2\,u(t)$

e) **Raised-cosine**

$\psi(t) = \sqrt{(2/3)}\,[\,1 - \cos(2\pi t / Tc)\,]\,u(t)$

3 Results and Analysis

Simulation experiments are conducted to quantify the influence of chip waveform selection on BER performance across both synchronous and asynchronous DS/SSMA configurations. Each simulation scenario involves K = 9 concurrent users employing spreading sequences of length N = 31 chips, ensuring a consistent basis for comparative analysis. The BER evaluation covers three spreading code strategies—random sequences, best-case Gold codes, and worst-case Gold codes—combined with three chip pulse profiles: rectangular, Blackman, and Lanczos waveforms.

BER performance curves comparing both best-case and worst-case Gold code selections against random spreading codes for the *synchronous* case are presented in Figure 1. The best-case Gold sequence configuration achieves substantially lower BER than the random code baseline, whereas the worst-case Gold configuration exhibits degraded performance relative to the randomly coded system. Statistical error bars in Figure 1 confirm that these observed differences are significant across all tested *Eb/No* values tested.

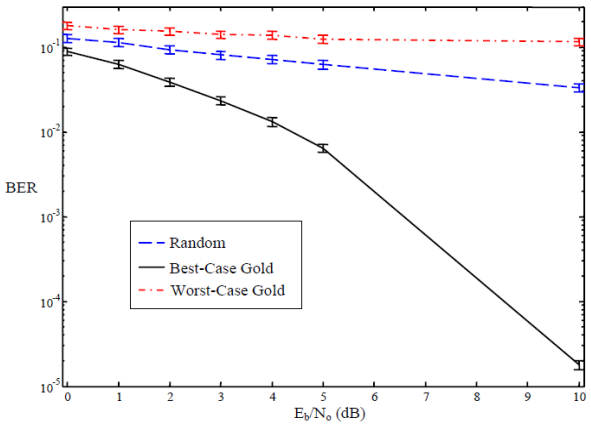


Fig. 1: Synchronous Network: Gold vs. Randomly Coded System

Source: created by the authors

An analogous BER comparison between best-case and worst-case Gold codes and random spreading codes for the *asynchronous* case is depicted in Figure 2. The same trend holds: best-case Gold codes yield improved BER while worst-case Gold codes underperform the random baseline. The error bars confirm statistical significance of this gain at *Eb/No* values exceeding 1.0 dB. Notably, the magnitude of improvement attributed to Gold coding is comparatively smaller in the *asynchronous* system are less than observed for the *synchronous* scenario than in its synchronous counterpart. This behavior indicates that the favorable correlation structure inherent to Gold code families—encompassing both their cross-correlation and autocorrelation properties—is optimally exploited under the *synchronous* case considered.

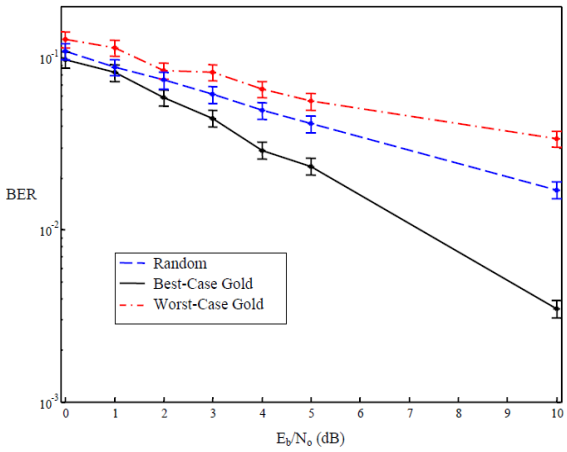


Fig. 2: Asynchronous Network: Gold vs. Randomly Coded System
Source: created by the authors

3.1 Synchronous System Performance

Figure 3, Figure 4, and Figure 5 present the BER outcomes for synchronous DS/SSMA systems across different chip waveform selections. In all three cases, the variation in pulse shape produces negligible BER improvement; the overlapping error bars confirm that the observed performance differences do not reach statistical significance.

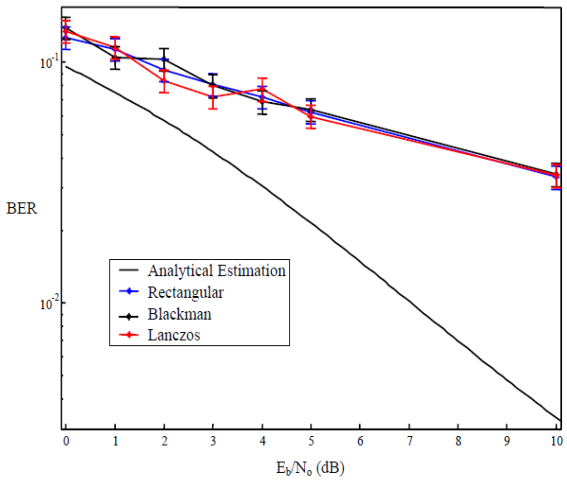


Fig. 3: BER for Synchronous Randomly Coded DS/SSMA System with K = 9 Users, N = 31 Length Codes and Chip Waveform Shaping
Source: created by the authors

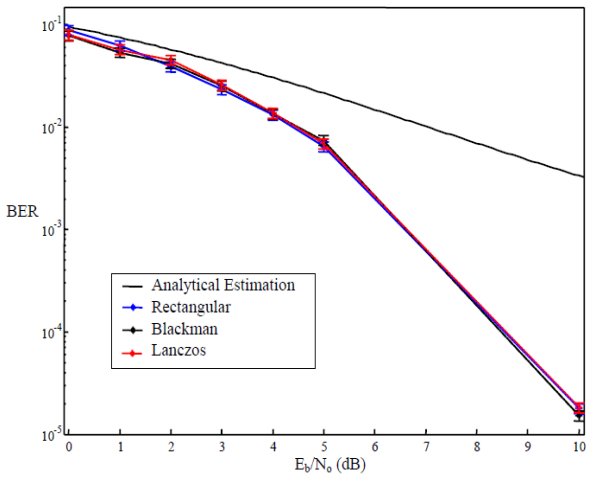


Fig. 4: BER for Synchronous Best-Case Gold Coded DS/SSMA System with K = 9 Users, N = 31-Length Codes and Chip Waveform Shaping
Source: created by the authors

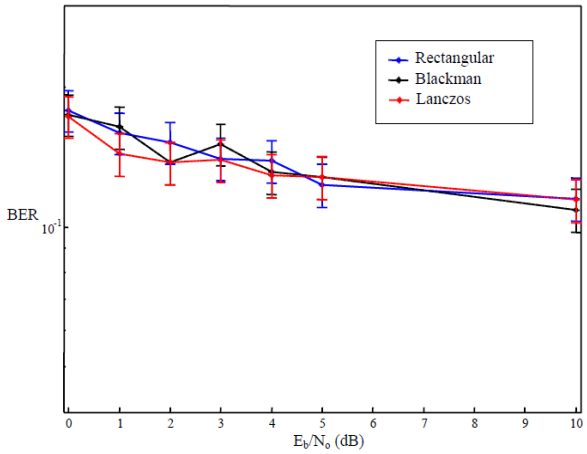


Fig. 5: BER for *Synchronous* Worst-Case Gold Coded DS/SSMA System with K = 9 Users, N = 31 Length Codes and Chip Waveform Shaping
Source: created by the authors

3.2 Asynchronous System Performance.

Figure 6 presents BER results for the asynchronous configuration with randomly coded spreading sequences. A clear advantage of the Lanczos chip pulse over the rectangular baseline is observed, with a gain of roughly 6.0 dB. Similarly, as shown in Figure 7, the best-case Gold coded asynchronous system also benefits from the Lanczos waveform, yielding an approximate 4.5 dB BER improvement. Figure 8 further reveals that when worst-case Gold sequences are deployed in the asynchronous setting, the Lanczos waveform provides the largest gain of approximately 7.5 dB.

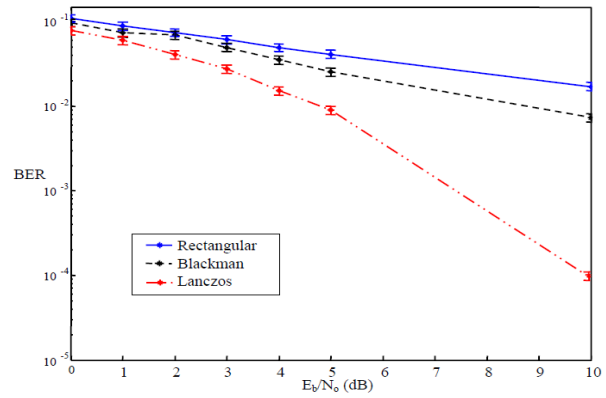


Fig. 6: BER for Asynchronous Randomly Coded DS/SSMA System with K = 9 Users, N = 31 Length Codes and Chip Waveform Shaping
Source: created by the authors

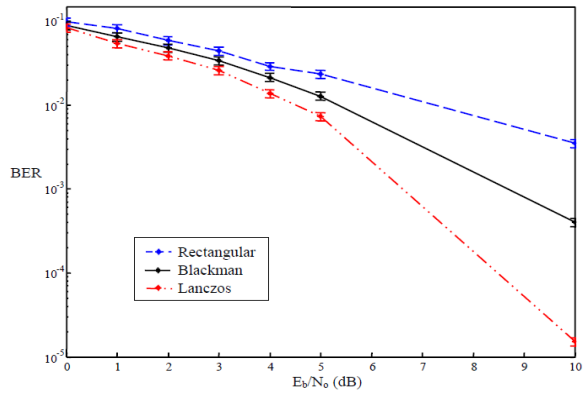


Fig. 7: BER for Asynchronous Best-Case Gold Coded DS/SSMA System with K = 9 Users, N = 31 Length Codes and Chip Waveform Shaping
Source: created by the authors

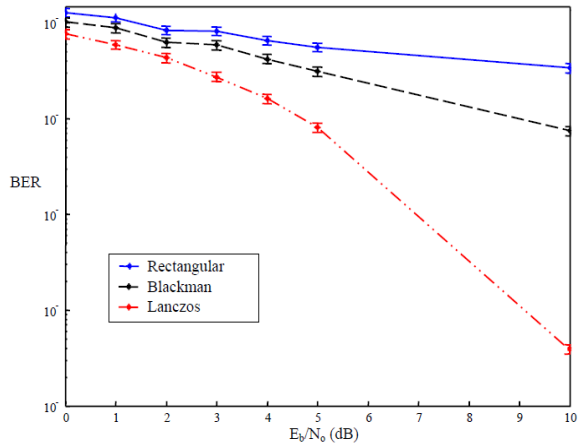


Fig. 8: BER for *Asynchronous* Worst-Case Gold Coded DS/SSMA System with K = 9 Users, N = 31 Length Codes and Chip Waveform Shaping
Source: created by the authors

4 Conclusions

This study presents a comprehensive simulation-based investigation into how multiple access interference (MAI) influences the performance of direct-sequence spread-spectrum multiple access (DS/SSMA) systems. Three primary system variables are examined: the choice between random and Gold spreading codes, the selection of chip pulse waveform shape, and variations in spreading code length. The findings shed light on the reliability of BER approximation methods and clarify the degree to which each parameter governs overall system behavior.

Random versus Gold Spreading Codes

Among the evaluated DS/SSMA configurations, systems utilizing Gold spreading codes consistently outperform those using randomly selected codes.

The performance advantage becomes most apparent at Eb/No levels above 1.0 dB, a threshold beyond which MAI-driven BER degradation overtakes the influence of AWGN. Moreover, the benefit of Gold codes is especially pronounced under synchronous network conditions, suggesting that the superior correlation structure of Gold code families is most effectively leveraged when all users are time-aligned.

Chip Waveform Shaping

The BER gains attributable to alternative chip waveform profiles are found to be concentrated predominantly in asynchronous operation. In the asynchronous case, symbol boundary offsets among users alter the spreading code cross-correlation characteristics relative to the synchronous scenario, opening an avenue for waveform-based interference reduction. When users experience fixed, known propagation delays in the synchronous case, the shift in BER—whether improvement or degradation—is largely governed by the corresponding change in cross-correlation variance introduced by the new chip pulse shape. A reduction in this variance translates directly into lower MAI power and, consequently, improved BER outcomes as the chip waveform profile is adjusted.

Declaration of Generative AI and AI-assisted Technologies in the Writing Process

During the preparation of this work, the author(s) utilized artificial intelligence (AI) technologies solely for the purpose of linguistic refinement and grammatical correction. Following the application of these tools, the author(s) comprehensively reviewed, verified, and edited the resulting text. The author(s) maintain full accountability and responsibility for the accuracy, integrity, and final content of the publication.

References:

[1] Cho, Joon H. and James S. Lehnert. "Optimum Chip Waveforms for DS/SSMA Communications with Random Spreading Sequences and a Matched Filter Receiver," Wireless communications and Networking Conference, 1999. 574-578. Septemebr 1999.

[2] Geraniotis, Evaggelos and Behzad Ghaffari. "Performance of Binary and Quaternary Direct-Sequence Spread-Spectrum Multiple-Access Systems with Random Signature Sequences," IEEE Transactions on Communications, 39(5): 713-724 May 1991.

[3] Jain, Raj. The Art of Computer Systems Performance Analysis. New York: John Wiley & Sons, Inc., 1991.

[4] Kok, Boon K. and M. A. Do. "Effects of Spreading Chip Waveform Pulse-Shaping on the Performance of DS-CDMA Indoor Radio Personal Communication Systems in a Frequency-Selective Rician Fading Channel," IEEE International Symposium on Consumer Electronics. 198-201. December 1997.

[5] Lehnert, James S. Final Report on Phase One Activities. Tactical Targeting Network Technologies Subcontract No. 4400-00-3308. September 2002.

[6] Leon-Garcia, Alberto. Probability and Random Processes for Electrical Engineering. Reading, Massachusetts: Addison-Wesley, 1994.

[7] Parl, S. "A New Method of Calculating the Generalized Q-function," IEEE Transactions on Information Theory, 26(1): 121-124 January 1980.

[8] Peterson, Roger L., Rodger E. Ziemer and David E. Borth. Introduction to Spread Spectrum Communications. New Jersey: Prentice Hall, 1995.

[9] Pursley, Michael B. "Performance Evaluation for Phase-Coded Spread Spectrum Multiple Access Communication-Part I: System Analysis," IEEE Transactions on Communications, 25(8): 795-799 August 1977.

[10] Yao, Kung. "Error Probability of Asynchronous Spread Spectrum Multiple Access Communication Systems," IEEE Transactions on Communications, 25(8): 803-809 August 1977.

Contribution of Individual Authors to the Creation of a Scientific Article (Ghostwriting Policy)

J. Ravindra Babu, Problem identification
K Sai Sankar, Literature review
V Lahari[3], Different methods identified
Sk Noor Ahamad, Drafting
K Srinivas, Solution identified
J V Ravi Chandra, Carried out the simulation with Matlab
J V Ravi Teja, Algorithm implementation
G Srujana, responsible for documentation

Sources of Funding for Research Presented in a Scientific Article or Scientific Article Itself

No funding was received for conducting this study.

Conflict of Interest

The authors have no conflicts of interest to declare that are relevant to the content of this article.

Creative Commons Attribution License 4.0 (Attribution 4.0 International, CC BY 4.0)

This article is published under the terms of the Creative Commons Attribution License 4.0
https://creativecommons.org/licenses/by/4.0/deed.en_US